CFD Letters

Journal homepage:
https://semarakilmu.com.my/journals/index.php/CFD_Letters/index
ISSN: 2180-1363

Comparison Between Experimental Life Road Simulation and Computational Fluid Dynamics and Fluid Structure Interaction for Sedan Car

Bassem Nashaat Zakher[1,*], M. Elhadary[1], M.A.El-Gohary[1], Ibrahim M. El Fahham[1]

[1] Faculty of Engineering, Alexandria University, Egypt

ARTICLE INFO

Article history:
Received 6 January 2022
Received in revised form 16 February 2022
Accepted 17 February 2022
Available online 24 February 2022

Keywords:
CFD; FSI; sedan car; experimental life road simulation

ABSTRACT

The flow around road vehicle is characterized by regions of separation that affect the aerodynamics and performance of the vehicle due to the variations in the negative pressure zones. In this work, Computational fluid dynamics and Fluid-structure interaction models are developed to simulate the aerodynamic performance of a sedan car. An experimental live road simulation is conducted to validate the performance and the accuracy of the presented models. The experimental setup was organized on a sedan car using tufts and digital cameras for flow visualization. Four cruise speeds of 40, 60, 80, and 100 km/hr are used. At low cruise speed the FSI simulation can attain the required result for indicating the negative pressure zones, created behind the car tail and mostly close to the car body. The experimental results appear to visualize the movement of the tufts that attained a certain angle corresponding to the flow speed, which matches the distribution of negative pressure and wake area. At high cruise speed the CFD simulation elucidated the separation area where the negative pressure created behind the car tail matched the movement of the tufts which attained an approximate straight angle corresponding to the flow speed having a swirling movement.

1. Introduction

The flow generated by the movement of a road vehicle is extremely complex. In contrast to the flow around aeronautical configuration, the road vehicle flow is characterized by regions of separation both small and large which can be of an open or closed type and may exhibit quasi-two dimensional or fully three-dimensional structures [1]. Large areas of separated flow are present at the trailing perimeter of the vehicle body and on the underside where the flow is disturbed by mechanical and structural elements and by the rotating wheels. A feature of the environment in which a road vehicle operates is the ambient wind that is almost always present. The speed and path of the vehicle differ from that of the wind. In the resulting yawed flow, the wake and the local regions

* *Corresponding author.*
E-mail address: Bassem.zakher1@gmail.com (Bassem Nashaat Zakher)

https://doi.org/10.37934/cfdl.14.2.8197

of separation are asymmetrically deformed, thus adding to the complexity of flow field, as shown in Figure 1.

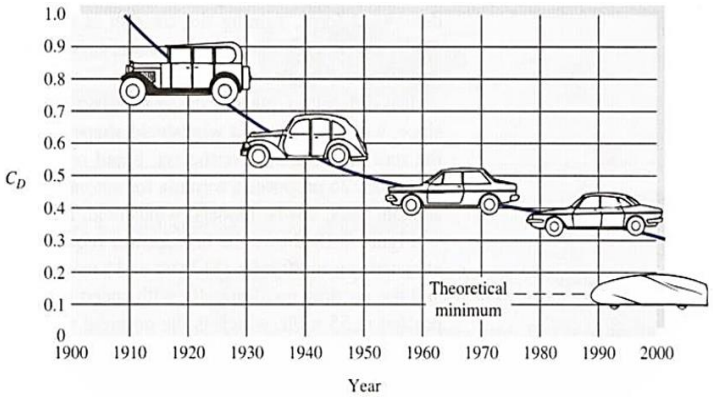

Fig. 1. Drag coefficient for different car shapes [1]

Temporal changes in the ambient conditions superimpose a time history on the phenomenon in addition to the inherent unsteadiness of separated flows [2]. Road vehicles move in close proximity to the ground and share common pathways, so that interaction between the overall flow-fields of vehicles of different shape and size during the passing and overtaking phases is a common occurrence. Flow passing over the vehicle underbody is restricted by the presence of the ground interaction between flows generated by the rough vehicle underbody wheels and the ground result in a complex viscous flow in this region [3]. The typical aerodynamic problems for road vehicles are the drag caused by flow separation and vortex formation, noise caused by flow separation and vortex formation directional sensitivity and instability caused by yaw along with side wind forces and gusts. Power consumption by proposed drag reduction devices and controls, excessive upper surface lift and increased download required are also problems required to be resolved.

Aerodynamics is a branch of dynamics concerned with studying the motion of air, particularly when it interacts with a moving object [4]. Aerodynamics is a subfield of fluid dynamics and gas dynamics, with much theory shared between them. Aerodynamics is often used synonymously with gas dynamics, with the difference being that gas dynamics applies to all gases. Understanding the motion of air (often called a flow field) around an object enables the calculation of forces and moments acting on the object.

Typical properties calculated for a flow field include velocity, pressure, density and temperature as a function of position and time [5]. By defining a control volume around the flow field, equations for the conservation of mass, momentum, and energy can be defined and used to solve for the properties. Aerodynamic problems can be identified in a number of ways. The flow environment defines the first classification criterion. External aerodynamics is the study of flow around solid objects of various shapes. Evaluating the lift and drag on an airplane, the shock waves that form in front of the nose of a rocket or the flow of air over a hard drive head are examples of external aerodynamics. Internal aerodynamics is the study of flow through passages in solid objects. For instance, internal aerodynamics encompasses the study of the airflow through a jet engine or through an air conditioning pipe.

The aerodynamics of vehicles has been studied since the 1920's and 1930's, thought only in recent times have the tools for studying them become so powerful. After looking at the forces that play the greatest role in determining a car's efficiency, it can be said that the shape of the car and its aerodynamics are of the almost importance in design [6]. The aim of the manufacturer is to build a car to the limits of the aerodynamics in a way that can be mass produced. To plan the most

aerodynamic car, researchers and designers pay attention to the shape of the front end, its underbody, its air ducts to the radiator, its compartment ventilation, its loading, the angle of the windshield, and all exterior obstacles. Thus, the aerodynamics must balance with the safety, stability and comfort of the passenger. Road vehicles are now the subject of extensive research on aerodynamic forces, both lift and drag. Better streamlining of car shapes has resulted over the years in the large decrease in the vehicle drag coefficient as shown for example Figure 1. Modern cars have an average drag coefficient of about 0.35, based upon the frontal area since the frontal area has also decreased sharply. The minimum drag coefficient has reached 0.15 for a tear-shaped vehicle, which can be achieved anytime the public is willing to purchase such a shape.

The “Ahmed” body model is a model for a simplified car, consisting of a sharp nose with rounded edges fixed onto a two legs middle section and a rear end with slanted surface, the angle of which can be changed. Studying the effect of changing the slant angle on drag coefficient for constant Reynolds number and the effect of Reynolds number on drag coefficient for different slant angles, As the rear slant angle increases, Zakher and Ammar [7] observed a decrease in drag coefficient until they reach the 23.5° slant angle which is a critical angle results in the minimum drag coefficient (Cd) of 0.37. For steeper slant angles of more than 30°, the flow over the rear slant become fully separated and the drag coefficient increased to 0.505. For Ahmed body, it is found that a slant angle of 25° gives minimum vortices formation irrespective of car speed and drag coefficient equals to 0.376 which is near the minimum value of C_d.

Many companies and laboratories have automotive wind tunnels, some full-scale and with moving floors to approximate actual dynamic similarity. The blunt shapes of most automobiles, together with their proximity to the ground cause a wide variety of flow and geometric effects. Simple changes in a part of the shape can have large influence on aerodynamic forces. However, to quantify the exact effect of geometric changes on automotive forces, for example changes in a windshield shape might interact with downstream flow over the roof and trunk. A two-dimensional model for a sedan car was developed by Sivaraj *et al.,* [8] using ANSYS Fluent software and was compared to existing results in the literature. VGs installed at the sedan's rear end are found to improve the Aero characteristics with a height of 25 mm. VGs having a height of 25 mm are found to improve the Aero characteristic of the car rear in general. It is concluded here that there is nothing that can be considered as the optimum design for the car rear shape to cover the whole range of car speed. VGs are recommended to be installed for higher car speeds, while the original design is preferred for lower car speeds.

To achieve high fuel efficiency, vehicles designs are inclined to choose lightweight materials and structures. However, these structures are generally weak, and structural integrity is a common concern. Tiew *et al.,* [9] proposed a set of economic materials and carried out a fluid structure interaction (FSI) study in one-way coupling analysis on a Shell Eco-Marathon (SEM) prototype car which travels in a low-speed range to analyze its structural response. The fully assembled SEM prototype car was analyzed with ANSYS Workbench in the coupling of the fluid and structural solver in a one-way FSI. Their proposed material only experiences minimum deformations. From both the deformation and stress analysis, they found out that the proposed material set is safe to be used in SEM car designs and eco-friendlier than the common materials.

Premoli *et al.,* [10] discussed the simulation of Computational fluid dynamics that are used to study the effect of the relative motion between train and infrastructure scenarios to analyze the differences that occur in wind tunnel tests between stationary and moving vehicles. Their numerical model is used to study the effects of the relative motion between the train and infrastructure model or STBR. It was concluded that even if static tests are not conservative, to obtain the differences in terms of

CWC significantly low in the STBR scenario and these results support the adoption of still model tests on STBR scenario as representative of train aerodynamics.

Studying drag force modifiers in passenger vehicles, Patil *et al.,* [11] investigated the fluid structure interaction that exists in airflow contact with passenger car chin spoilers. Their main objective was to study the deformation of chin spoilers as a result of the air pressure and its effect on the drag force changes. On the other hand, Kant *et al.,* [12] introduced a valuable review about the use of FE tools such as “Fluent” to study the effect of drag force on both sedan and hatchback cars. He also studied the utility of using drag force modifiers such as spoilers and vortex generators on car stability and performance.

Brandt *et al.,* [13] affirmed that crosswinds affect the stability of vehicles, and their influence increase with driving speed. To improve high-speed driving stability, recent important research using unsteady aerodynamics and vehicle dynamics is necessary. Their study showed the importance of the positioning of the C.G, the aerodynamic coefficient of yaw moment, wheelbase, vehicle mass, and yaw inertia. Moreover, the axles' side force steer gradients and other suspension parameters revealed high potential in improving the stability of crosswind.

Krämer *et al.,* [14] concluded that while planning a new construction of a bridge the risk of traffic accidents due to critical wind conditions should be considered carefully. The determination of aerodynamic forces and moments on vehicles is indispensable for stability investigations. However, the aerodynamic coefficients of vehicle-bridge systems depend on many factors which make it difficult to generalize the procedure. Computational fluid dynamics modelling plays an important role in representing all possible wind flow angles and the relative motion between the vehicle and the bridge deck which remains difficult or rather hardly possible to perform in the wind tunnel.

Kamal *et al.,* [15] showed that the aerodynamic characteristics of a vehicle play a vital role in steering stability, performance, comfort, and safety of a car. Hence, the fuel efficiency is determined by the performance of the internal combustion engine and the aerodynamic design of the body. One of the most important aspects of automobile design is aerodynamic styling. A vehicle with low drag resistance provides advantages in terms of cost and efficiency. The study demonstrates the importance of having a car with suitable turbulence models that are appropriate to be applied for simulations in terms of its applicability, time effectiveness, and cost. The turbulence closure coefficients of any turbulence model were mainly calibrated using simple canonical flows. Those models may not work well for complex automotive flows with flow separations and attachments.

Bounds *et al.,* [16] investigated the influence of the SST k -w turbulence model closure coefficient values on the prediction veracity of force coefficients for three different geometries: NACA 4412 at 12 deg of attack, the Ahmed body model with 25 deg and 35 deg slant angles, and a real-life full-scale passenger car model. Their main finding was that the closure coefficient betta has the strongest influence on the prediction of drag and lift and, hence, the overall flow field.

Abobaker *et al.,* [17] showed that the Mesh type and quality play a major role in the accuracy and stability of numerical computation. They used ANSYS Fluent CFD software for a 2-D subsonic flow over NACA 0012 air foil at different angles of attack with structured and unstructured meshes. The effect of those mesh types on the drag and lift coefficients was investigated. Their results were also validated using experimental measurements for the selected air foil. The calculations the structured mesh showed favourable results as compared with experimental data.

The main aim of this research work is to study the effect of changing the cruise speed on the vehicle performance regarding the flow separation zones resulting from negative pressure which affects the car performance and the vehicle stability. A preliminarily theoretical prediction from the COMSOL software FSI module was first used followed by the CFD module to show the difference between the two modules and qualitatively elucidate the field experimental life road test results. The

results obtained from the experimental life road simulation is used to validate the simulation results and compare the results obtained from each module individually at different cruise speeds.

2. Methodology

2.1 Numerical Analysis

2.1.1 Introductory remarks on the sedan car body

We explore the use of software “COMSOL” [18] to find the CFD, FSI characteristics for the basic sedan body "Skoda Octavia A4”. Modification is proposed to cruise speed to minimize the external aerodynamic drag and to maximize the car stability. The efficiency of a CFD, FSI simulations depends, therefore, on the time span required to achieve the first set of results, as well as, the accuracy of the simulated flow quantities. The turns around time and confidence level in the predictions are two major criteria for success that complete with one another. Creation of the model geometry, discretization of the physical domain, and choice of a suitable numerical computing scheme are significant factors that can determine the level of success of such an effort.

The Octavia sedan car body model, having the dimensions given in Figure 2, has a projected area of 7.8061 m^2.

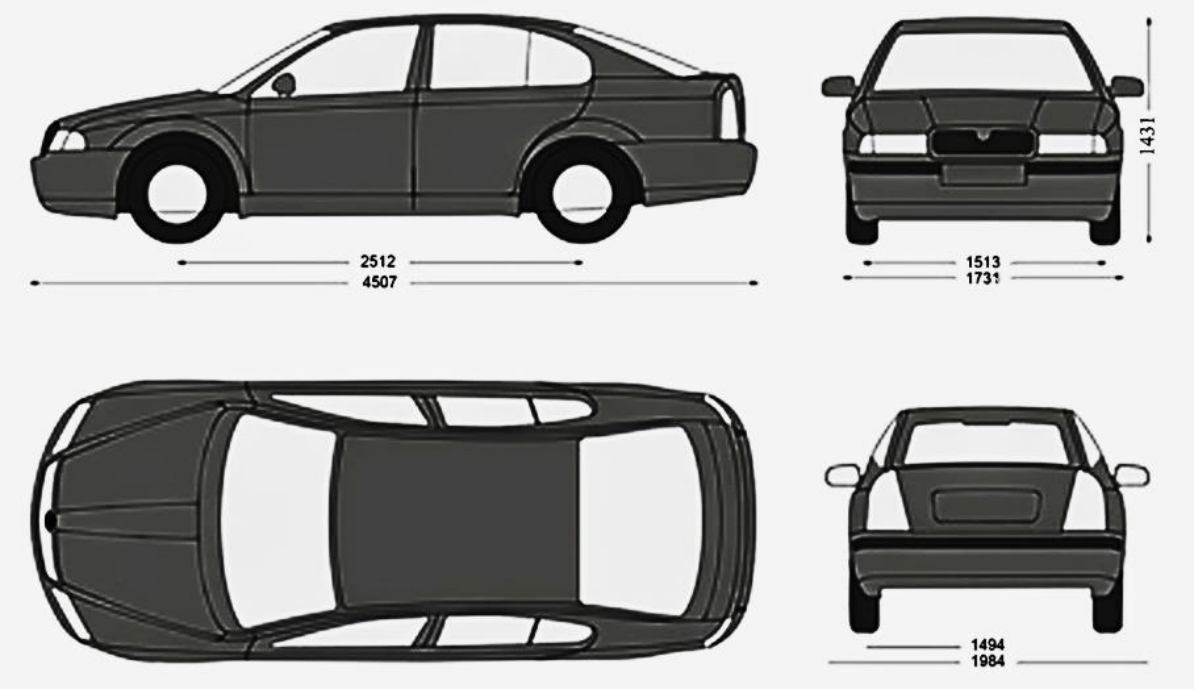

Fig. 2. the geometry description for sedan car model "Octavia A4"

The geometry used to simulate the sedan car was created using AutoCAD software package.

2.1.2 Domain and Mesh Grid description for the sedan car body

The grid was created for the prepared geometry by using COMSOL software package. COMSOL supports various mesh types and allows the user to solve one-way or two ways coupling fluid structure interaction also allows the user to refine or coarsen any grid based on the flow solution. The mesh is of structure type and it was made of free triangular cells. Moreover, the cells were clustered in the car trim area, where large gradients of flow parameters are expected. The Mesh grid for the flow domain around the sedan car is shown in Figure 3. The grid defines the boundaries of

the control volumes, while the computational node lies at the center of the control volume. The advantage of FVM (finite volume method) is that the integral conservation is satisfied exactly over the control volume.

As a 2-D model, the stream wise direction of the body section was kept in the mid plane of the car. The aerodynamic forces on the body are the result of complex interactions between flow separations and the dynamic behavior of the released vortex wake. The principal contribution to drag experienced by the car is the pressure drag, the rear of the vehicle provides the major contribution to pressure drag, so the rear design is critical in determining the mode of the wake flow and hence the drag experienced by the vehicle.

Because the flow is turbulent near the wall treatment the simulation becomes important. The turbulent models in COMSOL cannot be taken all the way to the wall of the boundary. Thus, the first node must be chosen above the laminar and buffer layer and in the logarithmic layer.

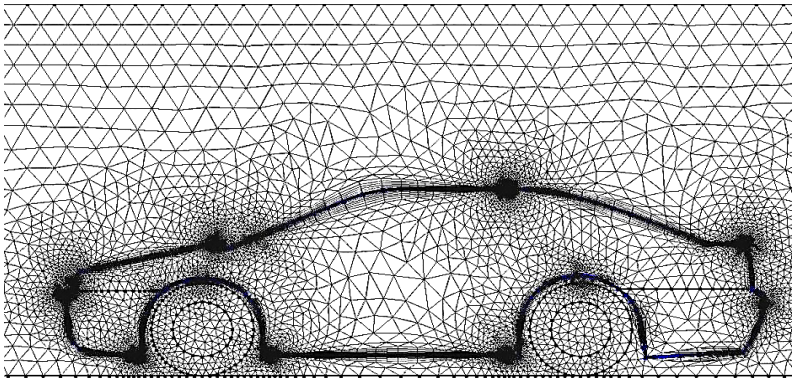

Fig. 3. The Mesh grid for the flow domain around the sedan car

2.1.3 Boundary conditions
2.1.3.1 Inlet and outlet boundary conditions

The inlet boundary conditions implemented in this study were changed according to the state of the fluid flow velocity, the outlet boundary condition is constant in all state of study. Velocity inlet boundary condition has been used for the vehicle inlet, while pressure outlet boundary condition is used in the vehicle outlet. Inlet velocity varies from 11.1 to 27.8 m/s (40-100 km/h). The pressure outlet equal to zero-gauge pressure.

2.1.3.2 Wall boundary condition

Once the CAR geometry is successfully generated in COMSOL, boundary conditions are enforced on the required surfaces. The CAR is defined as a solid body with a wall boundary condition, the boundary zone for the sliding mesh. The mean velocity field is affected through the no-slip condition that has to be satisfied at the wall. The turbulence intensity is also changed by the presence of the wall. Very close to the wall, viscous damping reduces the tangential velocity fluctuations, while the normal fluctuation is also reduced. Toward the outer part of the near-wall region, however, the turbulence is rapidly augmented by the production of turbulence kinetic energy due to the large gradients in mean velocity.

2.2 Experimental Test Rig

The experimental test rig was designed to visualize the flow downstream of the road vehicle, using "SKODA OCTAVIA A4", as a field model with the help of flow tufts that simulate the flow at the rear end of the car [16].

The aim of the design is to achieve the following goals:

I. The flow at the rear end of the car is to be 2-D using two flow guides.
II. The provision of different cruising velocities for the car.
III. The movement and the shape taken by the tufts simulate the airflow.
IV. The tufts are used to simulate the flow downstream the rear end is attached on the rear slant body of the car where the back flow and the wake area are generated.
V. Recording the flow visualization of the tufts generated at the rear end of the car using two HD cameras.
VI. A gauze screen is fixed in the center of the rear slant part where the tufts are fixed to visualize the flow at the center of the back area and to record the behavior of the tufts over the boundary layer.
VII. To guaranty the flow is symmetric on the rear part of the car to prove the 2-D flow concept.
VIII. The experimental test rig allows the tufts to move in 2-D direction freely at different cruise speeds 20,40,60,80,100, km/hr.; to visualize the symmetry in flow at the rear slant part of the car, also to record the distribution of eddies at the wake area generated.

The test rig consists mainly of six main parts as follows:

I. The car (SKODA OCTAVIA A4), as shown in Figure 4 [16].
II. Two wood flow guides fixed from the front to the rear of the whole car body on the two sides of the car right and left, shown in Figure 4.
III. Flow tufts are made in two small rings ends with a straight tuft, as shown in Figure 5.
IV. Gauze screen made from stainless steel the dimension between the net is 10×10 mm, as shown in Figure 6.
V. Two HD- cameras, one is fixed on a self-stick at the rear slant part to record the behaviour of the tufts fixed there, and the second camera fixed in the right flow guide in a position normal to the gauze screen.
VI. Wires used to tight the parts used in the rig.

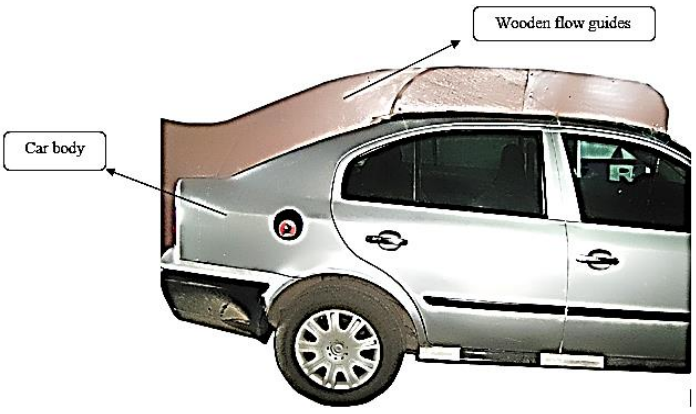

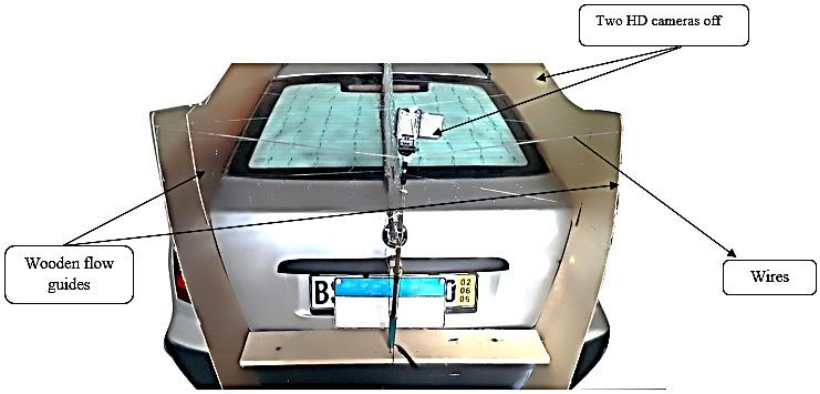

Fig. 4. The test rigs

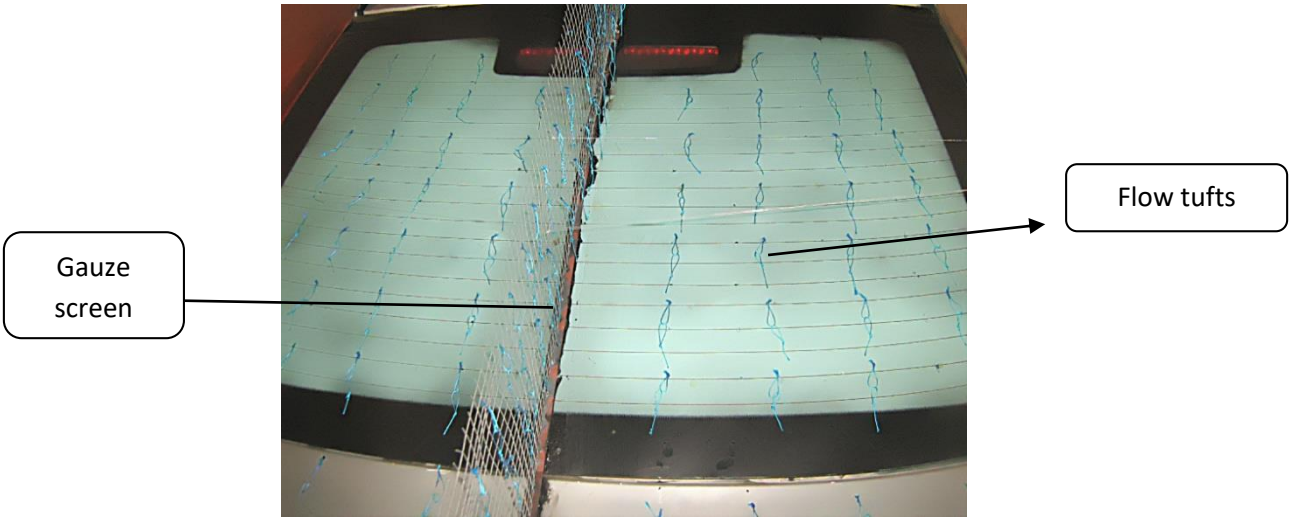

Fig. 5. Flow tufts

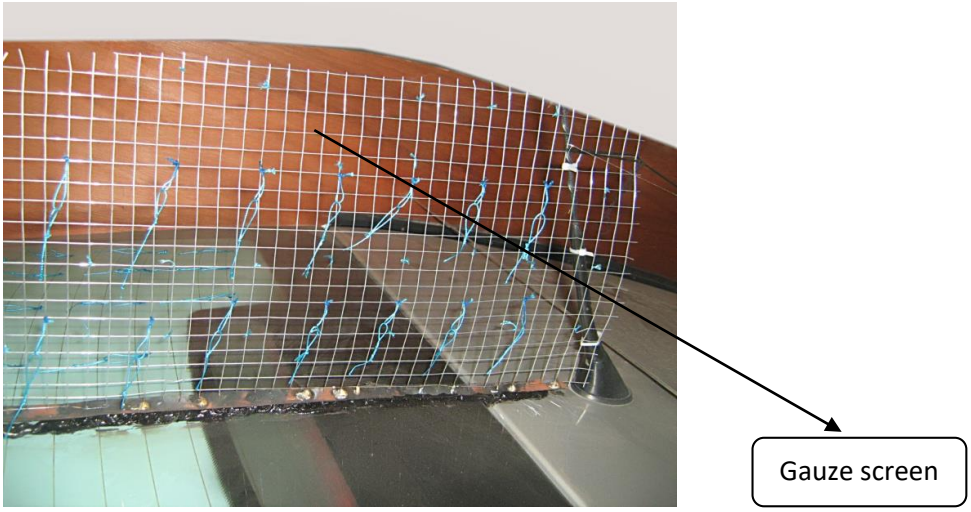

Fig. 6. Gauze screen with the tufts

2.3 The Experimental Car Model

The car used is "Skoda Octavia A4" as shown in Figure 2 and has the following parts:

2.3.1 Wood guides for the flow

They are being used to guide the flow around the car during the cruise speeds to be directely in 2-D. Also those guides help us to decrease the external effects as wind and other ways of distubing the flow around the car. The dimensions of those guides are 0.3 m height, 50 mm thickness and the rear part which covers the rear end is 0.75 m long. This part helps the flow at the rear to be guided in the wake area where the back flow and the eddies are formed. They are fixed from front to rear end with very thin robes and we use a rubber gaskect between the guides and the car body to be sure that they are tight fixed to decrease the leakage of air between the guides and the car body, Figure 7 shows the guide location and dimension.

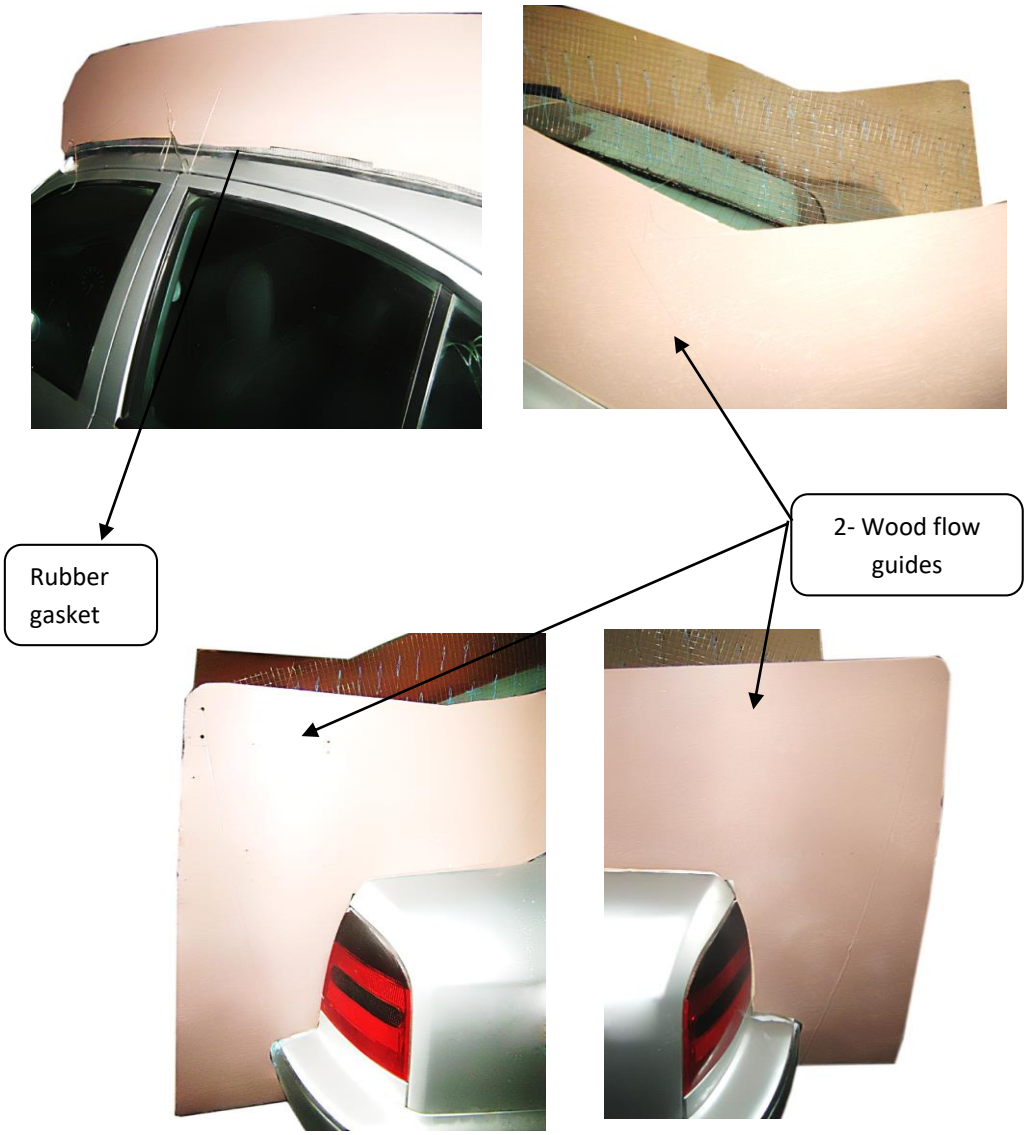

Fig. 7. Flow guides

2.3.2 The flow tufts

The flow tufts are made of silk cotton; they are designed of two rings ends with straight tuft. The two rings give the easy way of the tuft to rotate as the flow direction freely. The tuft length is 15 mm long for the straight part and the ring diameter is 12.5 mm. They are fixed on the rear slant part of

the car by an adhesive suitable for the silk cotton material to reduce the friction and the cross section of the point of adhesion, Figure 8 shows the tuft design and the point of adhesion.

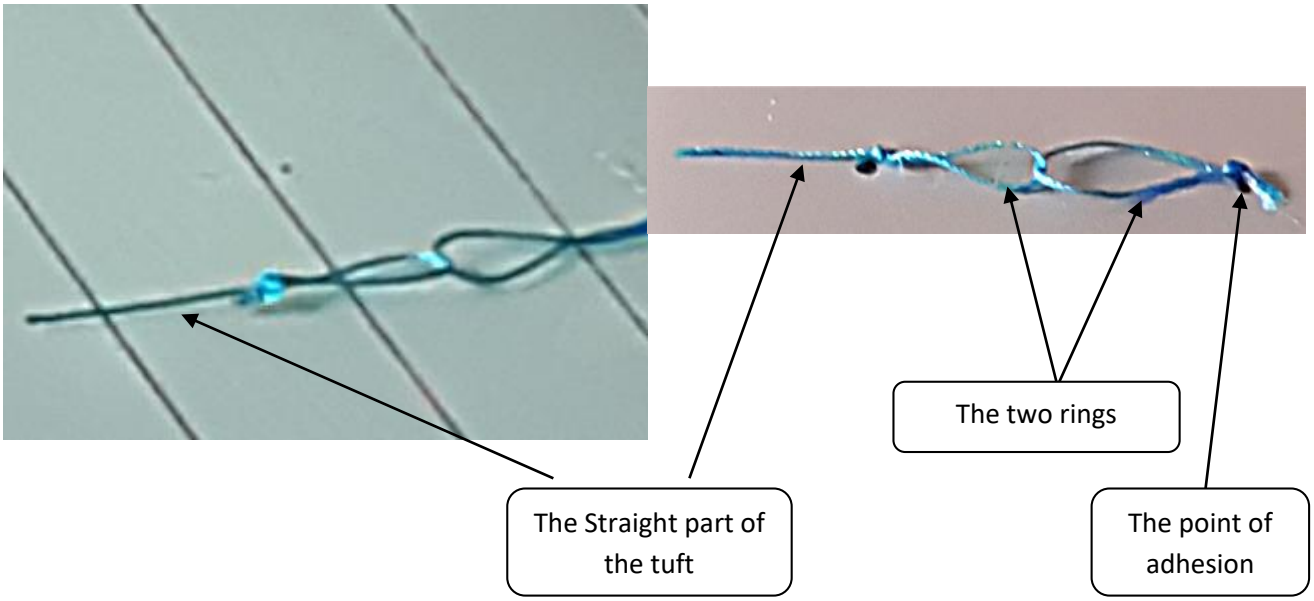

Fig. 8. Flow tufts

2.3.3 The gauze screen

The gauze screen is made of stainless steel has a dimension of each square equals to (10 mm × 10 mm), this type of gauze screen helps the flow around it to pass with minimum friction between air and the gauze screen body as shown in Figure 9. The location of the gauze screen is at the centre of the slant rear part of the car, this gives us the way to check the symmetry of the flow around the tufts located at the right and left sides of it. The gauze screen is fixed and stretched tightly from both ends with very thin ropes, between the gauze screen and the slant part we use silicon sealant with a thin layer to avoid the air leakage from the contact area between them, as shown in Figure 10. The tufts are fixed on the gauze screen to give us the flow profile at the area far from the boundary layer of the flow around the car body.

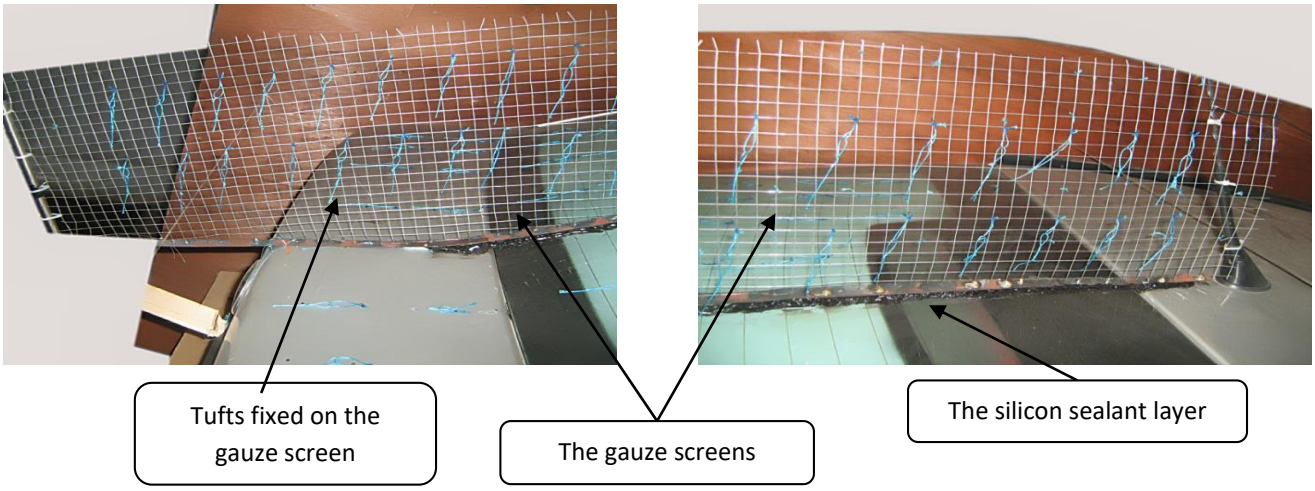

Fig. 9. Gauze screen and tufts installation

Fig. 10. Gauze screen cross section area

3. Results

The main objective is to investigate the validity for the assessment of vehicle aerodynamics, especially in the context of its possibility for aerodynamic forces. The method used is the flow visualization using “Flow Tufts” and applied to the full-scale vehicle "Octavia A4" with complicated geometry to qualitatively investigate the capability of capturing organized flow structures around the vehicle. As a result, it is demonstrated that flow visualization will be a powerful tool for the vehicle aerodynamic parameters (detecting the wake area behind the vehicle), in addition it can provide precious aerodynamic data. Visualizing and recording of the flow tufts behaviour at the gauze screen fixed in the centre of the rear area for different cruise speeds was employed to notify the flow pattern taken by the tufts to indicate the flow eddies formation.

The tufts fixed on the gauze screen visualize the flow pattern at the free stream, the behaviour of the flow at the wake area behind the vehicle. The flow on the gauze screen was recorded at two positions, one is normal to the gauze screen using an HD camera to record the flow behaviour at the free stream and the other position is at the end of the gauze screen to record the behaviour of the flow at the wake area. For the flow at the rear area an HD camera fixed to a self-stick near to the rear part was used to indicate and prove that the flow is symmetric and 2-D in addition to visualize and record the behaviour of the tufts at the rear area of the car where the eddies were formed, the tufts took the shape of the flow.

The experimental car was driven with different cruise speeds 20, 40, 60, 80 and 100 km/hr., in each speed the flow pattern was recorded and taken by the tufts at both areas (rear area and gauze screen), and a steady time was chosen to run the test to avoid the wind effects. The test was repeated several times to ensure that we have the same results of visualization.

3.1 Comparison between CFD, FSI Results from COMSOL and Experimental Results

3.1.1 At cruise speed of 40 km/hr

As increasing the cruise speed to 40 km/hr., the symmetry of the flow at the rear area of the car is clearly indicated. The tufts movement starts to increase one both right and left sections of the vehicle. Concerning the cruise speed (40 km/hr.), flow tufts attain an angle with a value greater than that of the previous speed. On the other hand, the tufts secured at first row are moving corresponding to the free stream, as shown in Figure 11(a). Regarding the CFD results resulted from "COMSOL" shown in Figure 11(b), it can be observed that the stream lines at the rear part of the

vehicle shown above at this cruise speed the wake area is slightly apart from the vehicle rear body area, comparing this result with the experimental images where the symmetry of the 2-D flow is proved and the movements of the tufts secured on the gauze attained a small angle corresponding to this low speed in the both upper and lower rows.

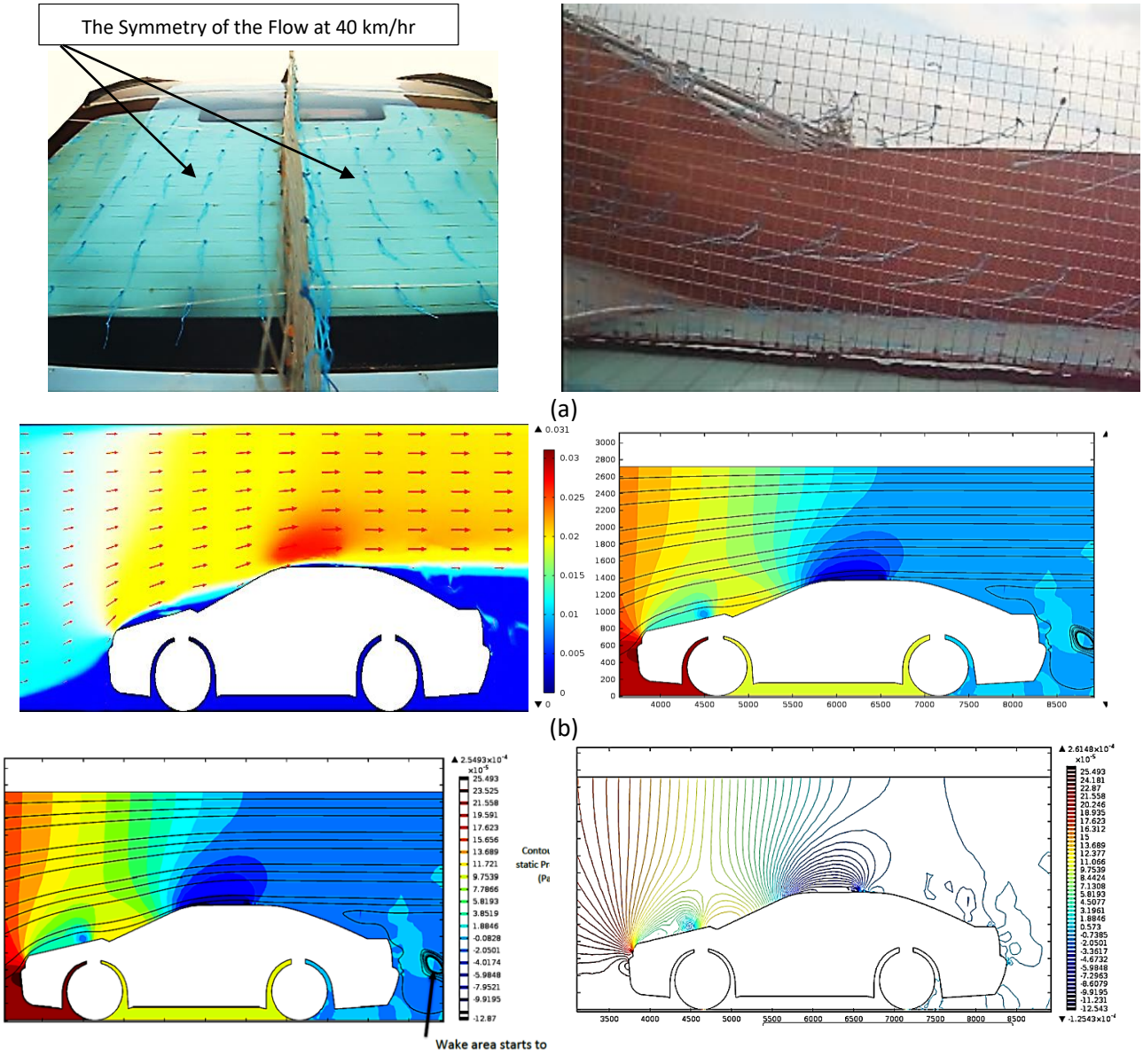

Fig. 11. (a) Experimental, (b) CFD, (c) FSI simulations for cruise speed of 40 km/hr

From the results above, it can be concluded that for this cruise speed the FSI simulation and CFD simulation are mostly the same regarding the velocity vectors and pressure contours. The results show that the CFD simulation can attain the required result for indicating the negative pressure zones, in addition the experimental results appear to visualize the movement of the tufts which matches the distribution of negative pressure and wake area.

3.1.2 At cruise speed of 60 km/hr

As increasing the cruise speed to 60 km/hr, the symmetry of the flow is indicated corresponding with the behaviour of tufts movement moreover the system of eddies formation starts to appear in more than one area comparing with the previous case of cruise speed of 40 km/hr. Those eddies are concentrated at the top of the rear end, while moving downwards the eddies are decreased due to the change of the contact surface area between the air flow and the rear part of the car as shown in Figure 12(a). In addition, the tufts secured on the gauze attained a steeper angle corresponding to this cruise speed in both upper and lower rows. And it can be observed that the system of vortices is starting to appear behind the tail of the vehicle and the velocity vectors are approximately as the angle attained by the flow tufts.

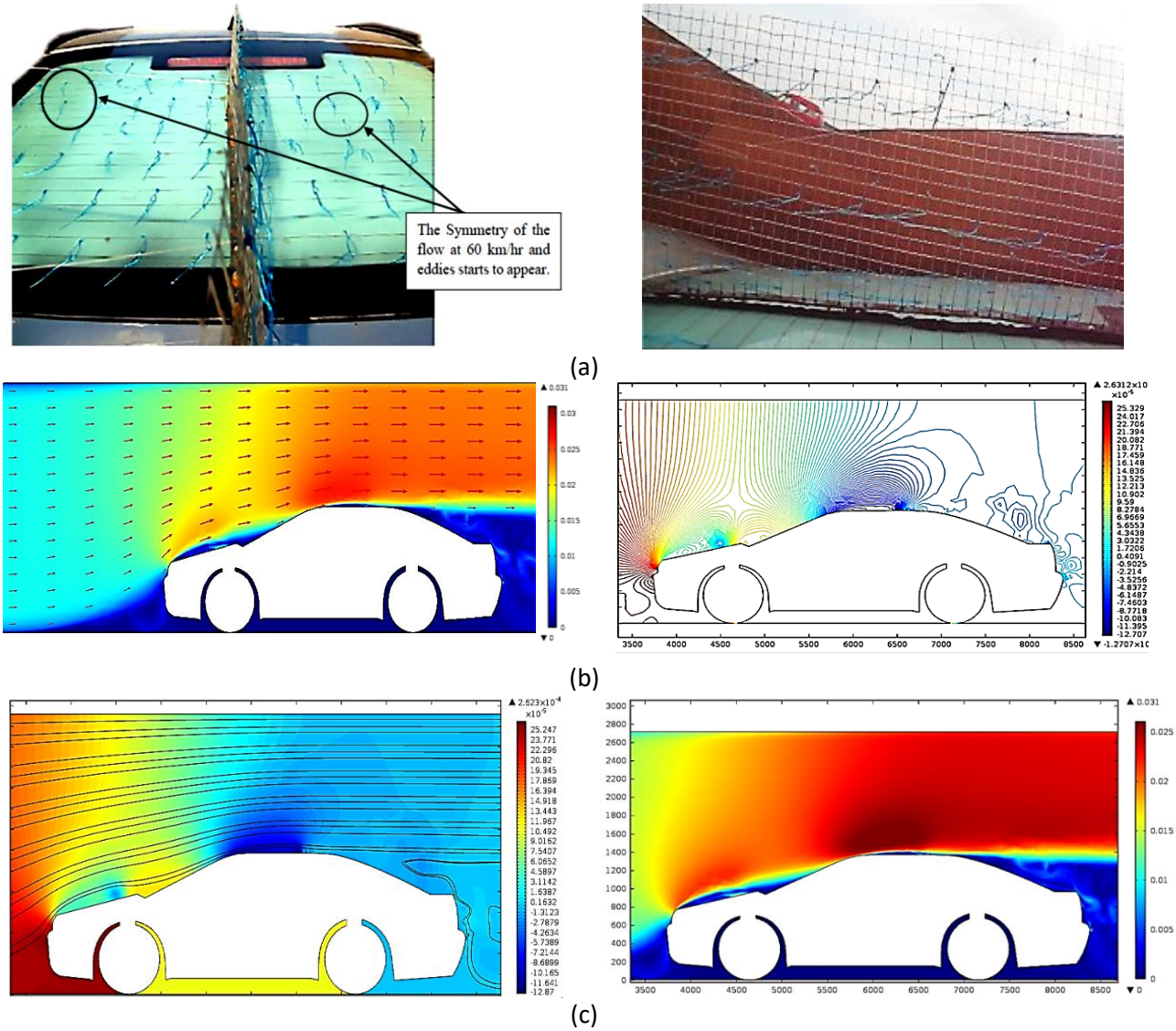

Fig. 12. (a) Experimental, (b) CFD, (c) FSI simulations for cruise speed of 60 km/hr

From the results above, it can be concluded that for this cruise speed the system of eddies formation starts to appear in more than one area comparing with the previous case of cruise speed of 40 km/hr., regarding the FSI simulation compared with the CFD simulation it can be shown that the FSI simulation can illustrate the wake area where the negative pressure created behind the car tail and mostly close to the car body, which matches with the experimental visualization that show

the tufts movement is attaining an angle corresponding to the flow speed which is approximately a straight angle for the tufts secured at the first row whose are related to the free stream.

3.1.3 At cruise speed of 80 km/hr

At the cruise speed of 80 km/hr., it can be observed that system of vortices is increasing, regarding the experimental images where the symmetry of the flow is proved, and the tufts secured on the gauze attained an approximate straight angle corresponding to this cruise speed in both upper and lower rows, as shown in Figure 13(a).

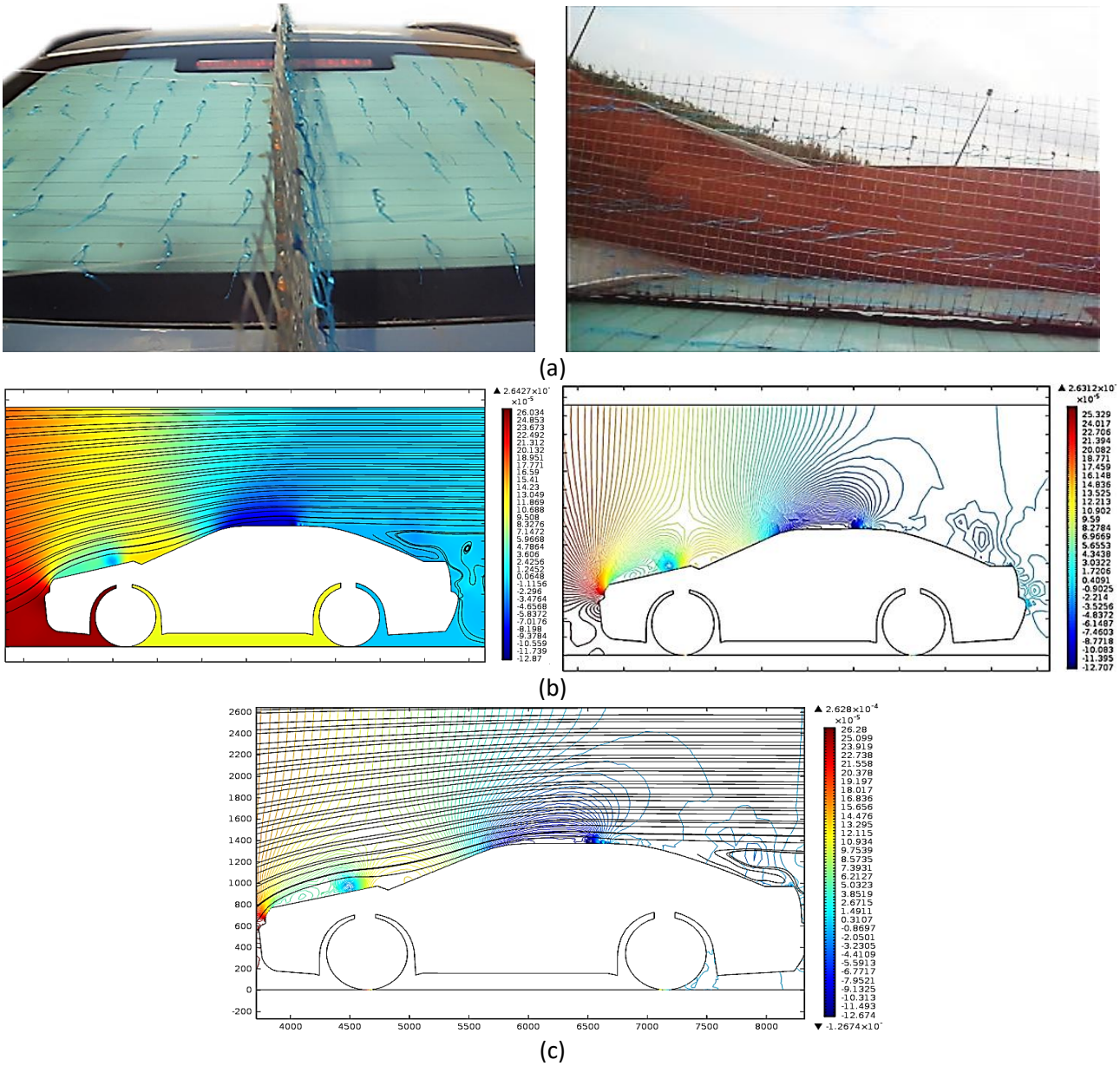

Fig. 13. (a) Experimental, (b) FSI, (c) CFD simulations for cruise speed of 80 km/hr

From the results above, it can be concluded that for this cruise speed the system of eddies formation increases to appear in more than one area comparing with the previous case of cruise speed of 60 km/hr., regarding the FSI simulation compared with the CFD simulation it can be shown that the CFD simulation can illustrate the separation area where the negative pressure created

behind the car tail and mostly close to the car body, which matches with the experimental visualization that shows the tufts movement is attaining an approximate straight angle corresponding to the flow speed This enables the main vortex to attain higher kinetic energy producing a region of lower pressure on the back side of the car and effectively increasing the drag force.

3.1.4 At cruise speed of 100 km/hr

For larger values of Reynolds number, as a cruise speed of 100 km/hr., the streamlines at the rear part of the vehicle is recording the system of vortices in more or less or the same in shape the kinetic energy associated with it, that is its strength increased considerably, as shown in Figure 14(a). Comparing this result with the experimental images where the tufts secured on the gauze attained a steeper angle corresponding to this cruise speed in the upper and lower rows. It can be concluded that although the system of vortices at different Reynolds number is more or less or the same in nature the opposing vortex generated in the wake zone is weaker at Re=8.5725×106 (100 km/hr.) than those at smaller and larger values of Re. This enables the main vortex to attain higher kinetic energy producing a region of lower pressure on the back side of the car and effectively increasing the drag force.

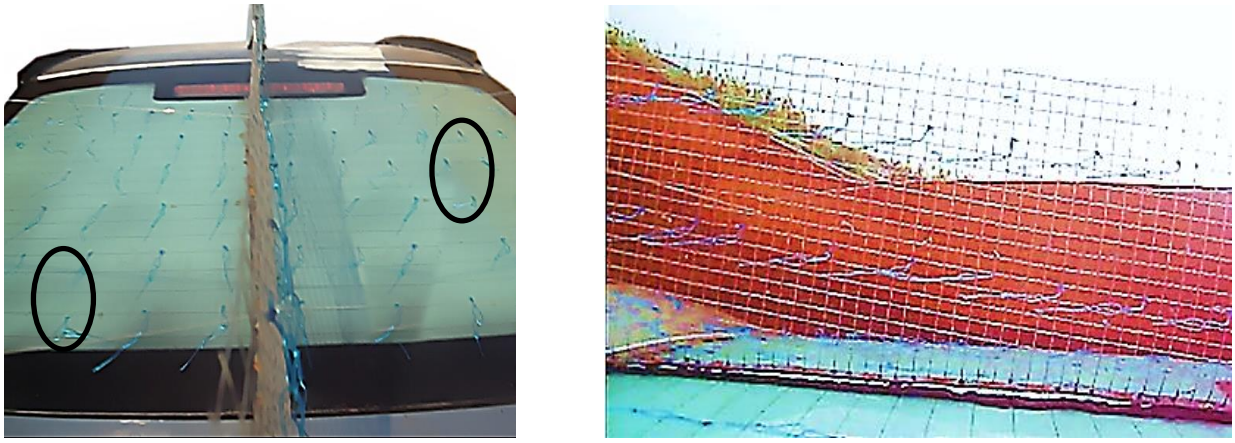

(a)

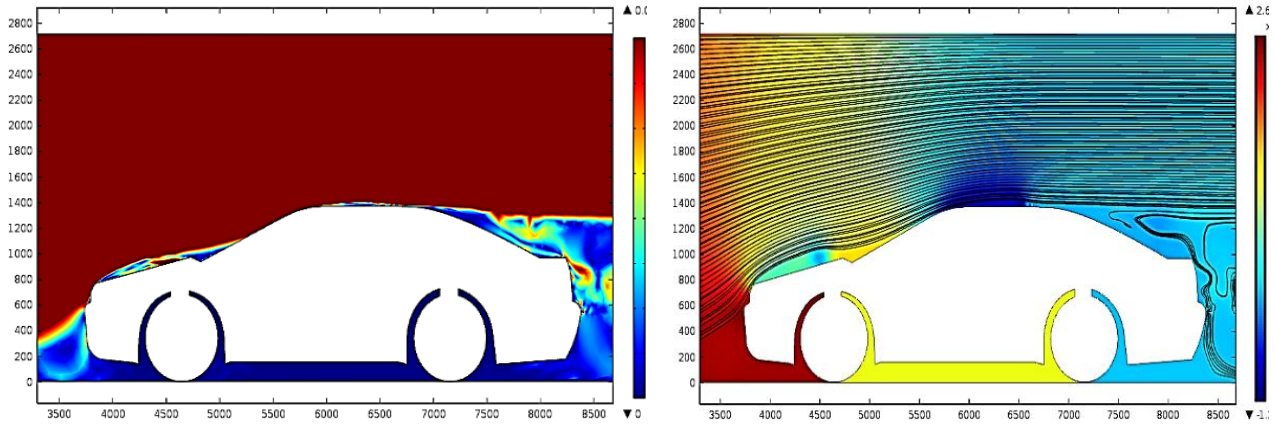

(b)

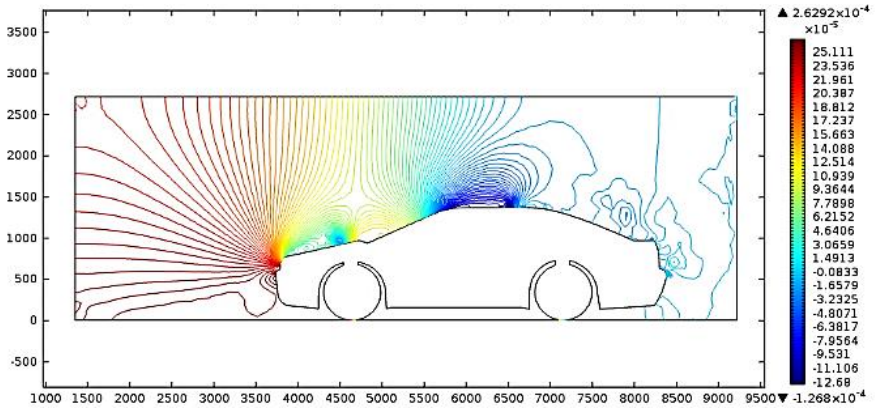

(c)

Fig. 14. (a) Experimental, (b) FSI, (c) CFD simulations for cruise speed of 80 km/hr

For this cruise speed the wake area increases comparing with the previous case of a cruise speed of 80 km/hr. Regarding the FSI simulation compared with the CFD simulation it can be seen that the CFD simulation can illustrate the separation area where the negative pressure created on car tail. Comparing both simulations with the experimental results, the tufts movement located at the rear end of the sedan car also have a swirl movement due to negative pressure.

4. Conclusions

The interaction of a fluid with a structure is an important phenomenon, particularly the interaction between a dynamic vehicle and the airflow. Computational fluid dynamics and Fluid structure interaction models are developed to simulate the performance of a sedan car. Also, an experimental live road simulation is conducted for a Skoda Octavia A4 sedan car to validate the performance and the accuracy of presented models at cruising speeds between 40 to 100 km/hr.

It was concluded that:

I. For a cruise speed of 40 km/hr., the CFD simulation can attain the anticipated results for indicating the negative pressure zones, as the experimental results appear to visualize the movement of the tufts which matches the distribution of negative pressure and wake area.

II. For a cruise speed of 60 km/hr., the FSI simulation can illustrate the wake area where the negative pressure created behind the car tail and mostly close to the car body, which matches with the experimental visualization that show the tufts movement is attaining an angle corresponding to the flow speed.

III. For a cruise speed of 80 km/hr., the CFD simulation can illustrate the separation area where the negative pressure created behind the car tail and mostly close to the car body, which matches with the experimental visualization that show the tufts movement is attaining an approximate straight angle corresponding to the flow speed, this enables the main vortex to attain higher kinetic energy producing a region of lower pressure on the back side of the car and effectively increasing the drag force.

IV. For a cruise speed of 100 km/hr., the CFD simulation can illustrate the separation area where the negative pressure created on car tail, comparing with the experimental result which shows the tufts movement located at the rear end of the sedan car have a swirl movement due to negative pressure.

Both models showed good agreement with the experimental results for different cruising car speeds.

Acknowledgement
This research was not funded by any grant.

References
[1] Munson, Bruce R., Alric P. Rothmayer, and Theodore H. Okiishi. *Fundamentals of Fluid Mechanics*. 7th Edition. Wiley , 2012.
[2] Hucho, Wolf, and Gino Sovran. "Aerodynamics of road vehicles." *Annual Review of Fluid Mechanics* 25, no. 1 (1993): 485-537. https://doi.org/10.1146/annurev.fl.25.010193.002413
[3] Happian-Smith, Julian, ed. An introduction to modern vehicle design. Elsevier, 2001.
[4] Muyl, Frédérique, Laurent Dumas, and Vincent Herbert. "Hybrid method for aerodynamic shape optimization in automotive industry." *Computers & Fluids* 33, no. 5-6 (2004): 849-858. https://doi.org/10.1016/j.compfluid.2003.06.007
[5] Corin, R. J., L. He, and R. G. Dominy. "A CFD investigation into the transient aerodynamic forces on overtaking road vehicle models." *Journal of Wind Engineering and Industrial Aerodynamics* 96, no. 8-9 (2008): 1390-1411. https://doi.org/10.1016/j.jweia.2008.03.006
[6] Zakher, Bassem Nashaat, Mostafa El-Hadary, and Andrew Nabil Aziz. "The Effect of Vortex Generators on Aerodynamics for Sedan Cars." *CFD Letters* 11, no. 6 (2019): 1-17.
[7] Zakher B., and Dalia M. Ammar. "The effect of changing the slant angle of Ahmeds car model on drag coefficient for different cruise speeds." *Journal of Recent Trends in Mechanics* 4, no. 1 (2019): 20-38.
[8] Sivaraj, G., D. Lakshmanan, and R. Veeramanikandan. "The computational analysis of sedan car with vortex generator." *International Journal of Advance Research in Science and Engineering* 4 (2015): 1531-1537.
[9] Tiew, Hedy Soon Keey, Ming Wei Lee, Chang Wei Shyang, Mohammad Hafifi Hafiz Ishak, and Farzad Ismail. "Fluid-Structure Interaction on The Design of Fully Assembled Shell Eco-Marathon (SEM) Prototype Car." *CFD Letters* 12, no. 12 (2020): 115-136. https://doi.org/10.37934/cfdl.12.12.115136
[10] Premoli, A., Daniele Rocchi, Paolo Schito, and G. Tomasini. "Comparison between steady and moving railway vehicles subjected to crosswind by CFD analysis." *Journal of Wind Engineering and Industrial Aerodynamics* 156 (2016): 29-40. https://doi.org/10.1016/j.jweia.2016.07.006
[11] Patil, Sunil, Robert Lietz, Sudesh Woodiga, Hojun Ahn, Levon Larson, Ronald Gin, Michael Elmore, and Alexander Simpson. *Fluid Structure Interaction Simulations Applied to Automotive Aerodynamics*. No. 2015-01-1544. SAE Technical Paper, 2015. https://doi.org/10.4271/2015-01-1544
[12] Kant, Shashi, Desh Deepak Srivastava, Rishabh Shanker, Raj Kunwar Singh, and Aviral Sachan. "A review on CFD analysis of drag reduction of a generic sedan and hatchback." *International Research Journal of Engineering and Technology (IRJET)* 4, no. 05 (2017): 973-982.
[13] Brandt, Adam, Bengt Jacobson, and Simone Sebben. "High speed driving stability of road vehicles under crosswinds: an aerodynamic and vehicle dynamic parametric sensitivity analysis." *Vehicle System Dynamics* (2021): 1-24. https://doi.org/10.1080/00423114.2021.1903516
[14] Krämer, V., B. Pritz, E. Tempfli, and M. Gabi. "Prediction of Aerodynamic Coefficients of Road Vehicles on Bridge Deck with and without Wind Protection by Means of CFD for Crosswind Stability Investigations." *Technische Mechanik-European Journal of Engineering Mechanics* 39, no. 1 (2019): 51-63.
[15] Kamal, Muhammad Nabil Farhan, Izuan Amin Ishak, Nofrizalidris Darlis, Daniel Syafiq Baharol Maji, Safra Liyana Sukiman, Razlin Abd Rashid, and Muhamad Asri Azizul. "A Review of Aerodynamics Influence on Various Car Model Geometry through CFD Techniques." *Journal of Advanced Research in Fluid Mechanics and Thermal Sciences* 88, no. 1 (2021): 109-125. https://doi.org/10.37934/arfmts.88.1.109125
[16] Bounds, Charles Patrick, Chunhui Zhang, and Mesbah Uddin. "Improved CFD prediction of flows past simplified and real-life automotive bodies using modified turbulence model closure coefficients." *Proceedings of the Institution of Mechanical Engineers, Part D: Journal of Automobile Engineering* 234, no. 10-11 (2020): 2522-2545. https://doi.org/10.1177/0954407020916671
[17] Abobaker, Mostafa, Sogair Addeep, Lukmon O. Afolabi, and Abdulhafid M. Elfaghi. "Effect of Mesh Type on Numerical Computation of Aerodynamic Coefficients of NACA 0012 Airfoil." *Journal of Advanced Research in Fluid Mechanics and Thermal Sciences* 87, no. 3 (2021): 31-39. https://doi.org/10.37934/arfmts.87.3.3139
[18] COMSOL Multiphysics Modeling Guide, by COMSOL AB. 2011.